Separating Solvation from Molecular Diffusion in Polymers

Yossef A. Elabd
Dept. of Chemical Engineering, The Johns Hopkins University, Baltimore, MD 21218

Timothy A. Barbari
Dept. of Chemical Engineering, University of Maryland, College Park, MD 20742

The diffusion of methyl ethyl ketone (MEK) in two vinyl alcohol/vinyl butyral (VA/VBu) copolymers (11- and 19-wt. % VA) was studied at low vapor activities using Fourier transform infrared-attenuated total reflectance (FTIR-ATR) spectroscopy. MEK has the ability to interact through hydrogen bonding to sites in the polymer and was chosen to study the effect of penetrant−polymer solvation on molecular diffusion. The assumption of local equilibrium was verified by examining the time-evolved concentrations of hydrogen-bound and free MEK determined from the carbonyl (C = O) stretching bands. A mathematical model that accounted explicitly for solvation during the diffusion process was developed. Solvation hindered the diffusion of MEK in the VA/VBu copolymer by factors of 2.0 (11-wt. % VA) and 2.6 (19-wt. % VA). After separating solvation from diffusion, true diffusion coefficients of MEK were compared to those of methylene chloride (CH_2Cl_2), a noninteracting penetrant of similar size to MEK. Within experimental error, true diffusion coefficients for MEK were the same as those for CH_2C1_2 over the concentration range studied.

Introduction

The literature contains several practical applications of diffusion in polymers with reversible binding between penetrant and polymer (solvation). Examples include drug−hydrogel interactions (Peppas and Wright, 1998; Sjöberg et al., 1999), doping of conducting polymers (Kim et al., 1988), and flavor-binding polymers (Harrison and Hills, 1997). To understand these applications for the design of optimal systems, a coupled approach using modeling and experiments is desirable. Hermans (1947) and Murphy et al. (1988) both solved this problem numerically under certain conditions, and more recently, Bartlett and Gardner (1996) presented a more unified treatment of the problem, examining all the possible limiting cases. In their study, under the local equilibrium (or diffusion-controlled) limitation, the equilibrium constant is the main driving factor in slowing or hindering diffusion, resulting in a lower overall diffusion coefficient. To combine these findings with experiment, a technique that can analyze quantitatively interactions between penetrant and polymer during the transport process is needed.

One technique of particular interest for the analysis of small-molecule diffusion in polymers is Fourier transform infrared-attenuated total reflectance (FTIR-ATR) spectroscopy (Fieldson and Barbari, 1995; Hong et al., 1997). The advantages of this infrared technique are its ability to examine multicomponent diffusion (Hong et al., 1998) and interactions between different penetrants (Barbari et al., 1996) and between penetrant and polymer (Elabd et al., 2000) through shifts in the infrared spectrum. In this study, the diffusion of methyl ethyl ketone (MEK) in two different vinyl alcohol/vinyl butyral (VA/VBu) copolymers (Figure 1) was studied. MEK has the ability to interact through hydrogen bonding to the polymer, and this interaction can be quantitatively determined through the carbonyl stretching vibration. Direct measurement of the concentrations of both free and hydrogen-bound MEK as a function of time allows the common assumption of local equilibrium to be tested and verified. The objective of this study was to use FTIR-ATR spectroscopy to determine both the equilibrium constant and true diffusion coefficient to understand the effect of penetrant−polymer solvation on the transport process. After ac-

Correspondence concerning this article should be addressed to T. A. Barbari.

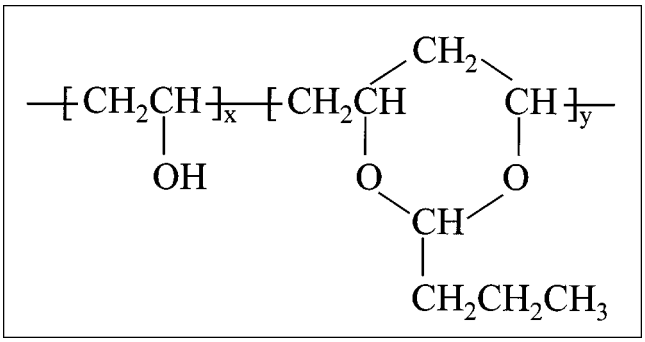

Figure 1. Structure of VA/VBu copolymer.

counting for solvation, the diffusion coefficient should be the same as that measured for a noninteracting molecule of the same size in the same polymer. This hypothesis will be tested here by comparing the true diffusion coefficient of MEK with that for methylene chloride.

Theoretical Development

Diffusion with solvation

Figure 2 depicts the diffusion process in a polymer with solvation, specifically for the system studied here. The penetrant, MEK, diffuses into a polymer with a low density of immobile hydroxyl groups (VA), with which MEK can solvate through hydrogen bonding. To describe this process mathematically, a diffusion model with a reversible binding equilibrium reaction was developed. The reaction between penetrant and binding site can be written as

$$A + B \underset{k_r}{\overset{k_f}{\rightleftharpoons}} AB, \tag{1}$$

where A, B, and AB represent the free penetrant (MEK), the polymer binding site (VA), and the hydrogen-bound MEK complex, respectively. The forward and reverse rate constants, are represented by k_f and k_r, respectively. The one-dimensional continuity equation for species A in a homogeneous film is

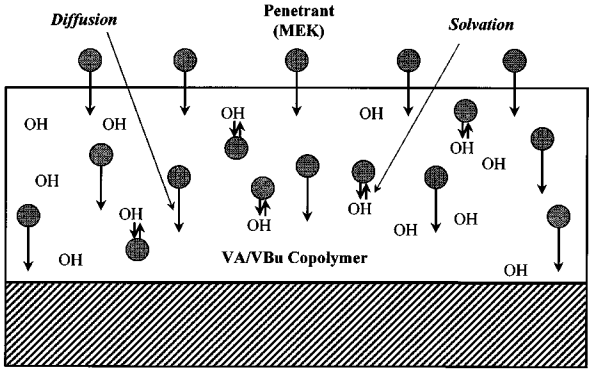

Figure 2. MEK diffusion in VA/VBu copolymer at a low density of hydroxyl groups (VA).

Hydrogen bonding interactions hinder the diffusion process.

$$\frac{\partial C_A}{\partial t} = D_A \frac{\partial^2 C_A}{\partial z^2} + r_A, \tag{2}$$

where z corresponds to the distance in the film, t represents time, C_A is the concentration of A (free MEK), and D_A is the diffusion coefficient of the free penetrant or true molecular diffusion coefficient. For a fixed number of sites, C_B^o, the rate of binding can be described by a Langmuir expression:

$$-r_A = k_f C_A C_B^o (1-\theta) - k_r C_B^o \theta, \tag{3}$$

where θ is the fraction of occupied sites, C_{AB}/C_B^o. The corresponding equation for hydrogen-bound MEK is

$$\frac{\partial C_{AB}}{\partial t} = C_B^o \frac{\partial \theta}{\partial t} = -r_A. \tag{4}$$

The model assumes that the hydrogen-bound form is immobile, or the activation barrier that must be overcome for hydrogen-bound MEK to execute a successful diffusion jump is much larger than that for a free MEK molecule ($D_{AB} \ll D_A$). Adding Eqs. 2 and 4 gives

$$\frac{\partial C_A}{\partial t} = D_A \frac{\partial^2 C_A}{\partial z^2} - C_B^o \frac{\partial \theta}{\partial t}. \tag{5}$$

If local equilibrium is assumed, an equilibrium constant can be written in terms of the concentrations of each species as

$$K = \frac{C_B^o \theta}{C_A C_B^o (1-\theta)}. \tag{6}$$

Equation 6 can then be substituted into Eq. 5 to derive a continuity equation for A in terms of C_A only (Bartlett and Gardner, 1996):

$$\frac{\partial C_A}{\partial t} = \left[\frac{(1+KC_A)^2}{(1+KC_A)^2 + KC_B^o} \right] D_A \frac{\partial^2 C_A}{\partial z^2}. \tag{7}$$

At low penetrant concentrations, the binding sites never reach saturation ($\theta \ll 1$), so Eq. 6 reduces to

$$KC_B^o = \frac{C_{AB}}{C_A} \tag{8}$$

and Eq. 7 becomes

$$\frac{\partial C_A}{\partial t} = \left(\frac{D_A}{1+KC_B^o} \right) \frac{\partial^2 C_A}{\partial z^2}. \tag{9}$$

For experiments conducted in this study, θ was in the range of 0.1 to 0.01 at equilibrium. If C_A in Eq. 9 is written in

terms of C_{AB} using Eq. 8, the following equation results:

$$\frac{\partial C_{AB}}{\partial t} = \left(\frac{D_A}{1 + KC_B^o} \right) \frac{\partial^2 C_{AB}}{\partial z^2}. \tag{10}$$

Equation 10 describes the time rate of change in hydrogen-bound MEK concentration written in terms of an apparent transport process. In other words, *AB* forms at the same rate as *A* diffuses owing to local equilibrium. Equations 9 and 10 describe the transport of free MEK in terms of an ''effective'' diffusion coefficient, defined as

$$D_{\text{eff}} = \left(\frac{D_A}{1 + KC_B^o} \right). \tag{11}$$

According to Eq. 11, solvation hinders the molecular diffusion process by the factor, $1 + KC_B^o$.

Diffusion coefficient measurement by FTIR-ATR spectroscopy

To determine the effective diffusion coefficient, Eqs. 9 and 10 can be written as

$$\frac{\partial C_i}{\partial t} = D_{\text{eff}} \frac{\partial^2 C_i}{\partial z^2}. \tag{12}$$

In Eq. 12, C_i is the concentration of either hydrogen-bound or free penetrant. The initial and boundary conditions for the ATR configuration (shown in Figure 3) are

$$C = 0 \qquad \text{at} \qquad 0 < z < L, \qquad t = 0 \tag{13}$$

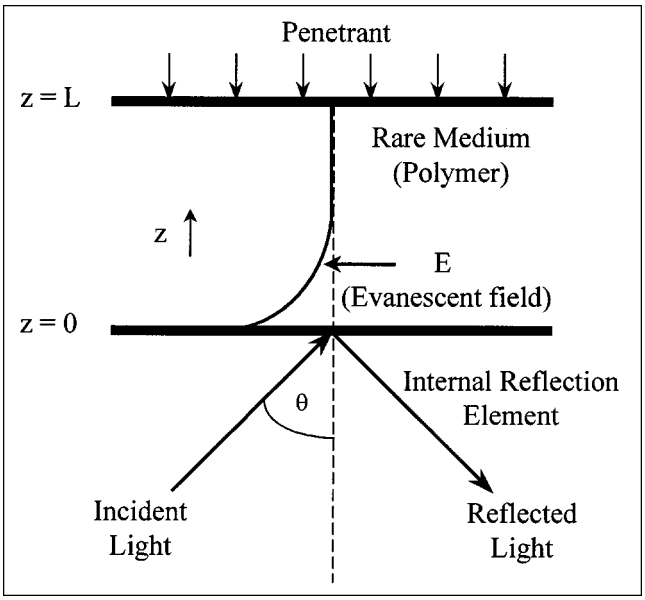

Figure 3. Experimental configuration of total internal reflection for studying diffusion in polymers.

$$\frac{\partial C}{\partial z} = 0 \qquad \text{at} \qquad z = 0, \qquad t \geq 0 \tag{14}$$

$$C = C_L \qquad \text{at} \qquad z = L, \qquad t \geq 0. \tag{15}$$

One solution to Eq. 12 with these boundary and initial conditions is given by

$$\frac{C}{C_L} = 1 - \frac{4}{\pi} \sum_{n=0}^{\infty} \frac{(-1)^n}{2n+1} \exp\left[\frac{D_{\text{eff}}(2n+1)^2 \pi^2 t}{4L^2} \right] \times \cos\left[\frac{(2n+1)\pi z}{2L} \right]. \tag{16}$$

Assuming weak infrared absorbance and negligible changes in the polymer refractive index (dilute solutions), concentration can be related to experimental infrared absorbance through the ATR differential form of the Beer-Lambert law (Harrick, 1965):

$$A = \int_0^L \epsilon^* C \exp\left(\frac{-2z}{d_p} \right) dz, \tag{17}$$

where A is the ATR absorbance, ϵ^* is an effective extinction coefficient for FTIR-ATR spectroscopy, and E_o is the field strength at $z = 0$. The depth of penetration, d_p, of the infrared radiation into the polymer film is defined as

$$d_p = \frac{\lambda}{2n_2\pi\sqrt{\sin^2\theta - \left(\frac{n_1}{n_2}\right)^2}}, \tag{18}$$

where n_1 and n_2 are the refractive indices of the polymer (listed in Table 1) and the ATR crystal (2.4 for zinc selenide), respectively; θ is the angle of incidence; and λ is the wavelength of absorbed light. Experimentally, the depth of penetration was much less than the polymer film thickness (L) in this study. Therefore, the concentration within d_p is not spatially variant to a significant degree, owing to the no-flux boundary condition, and Eq. 17 reduces to

$$A = \frac{1}{2} \epsilon^* d_p C(z = 0). \tag{19}$$

Equation 17 can then be rewritten in terms of the ATR ab-

Table 1. Molecular Weights, Refractive Indices, Densities, and Glass Transition Temperatures for VA/VBu Copolymers

VA Content (wt. %)	MW [GPC]	n_1	ρ (g/cm^3)*	T_g (°C)*
11	110,000	1.485	1.083	59
19	88,000	1.490	1.119	65

*Reimers et al. (1993).

sorbance with the use of Eq. 19:

$$\frac{A_t}{A_{\text{eq}}} = \frac{C(t,\, z=0)}{C_L} = 1 - \frac{4}{\pi} \sum_{n=0}^{\infty} \frac{(-1)^n}{2n+1} \times \exp\left[\frac{-D_{\text{eff}}(2n+1)^2 \pi^2 t}{4L^2} \right], \quad (20)$$

where A_t is the integrated infrared absorbance of the diffusing penetrant at time t, and A_{eq} is its value at equilibrium.

Equilibrium coefficient determination by FTIR-ATR spectroscopy

Additionally, the equilibrium constant in Eq. 8 can be rewritten in terms of absorbance as

$$KC_B^o = \frac{A_{AB}}{A_A} \left(\frac{\epsilon_A^* d_{p_A}}{\epsilon_{AB}^* d_{p_{AB}}} \right). \quad (21)$$

Other studies (Elabd and Barbari, 2000; Teo et al., 1997; Senich and MacKnight, 1980; Wang and Cooper, 1983; Sung and Schneider, 1978; MacKnight and Yang, 1973) have shown that effective extinction coefficients for hydrogen-bound and free carbonyl stretching groups are approximately equal, reducing Eq. 21 to

$$KC_B^o = \frac{A_{AB}}{A_A} \quad (22)$$

when the two depths of penetration are nearly equal, as they are here for the two carbonyl bands ($< 1\%$ difference). Values for KC_B^o can be determined from a linear regression of A_{AB} vs. A_A. The true diffusion coefficient, D_A, can then be determined from the effective diffusion coefficient (see Eq. 11), which is obtained by regressing the experimental normalized absorbances using Eq. 20.

Experimental

Materials and sample preparation

The two VA/VBu copolymers, 11- and 19-wt. % VA content, were purchased from Scientific Polymer Products, Inc., and contained 1 wt. % residual acetate groups. Table 1 lists the physical properties of the polymers, both of which are completely amorphous (Reimers et al., 1993). The film-casting solvent, 1-butanol, was purchased from Aldrich (15467-9) with a purity of 99.5%. In Table 2, the physical properties of the two penetrants, methyl ethyl ketone (Aldrich 27069-5), 99.5% purity, and methylene chloride (Fisher D37-1), 99.5% purity, are listed. The Lennard-Jones diameters, listed in Table 2, for MEK and CH_2Cl_2 were obtained from Brokaw (1969) and Braune and Linke (1930), respectively.

To obtain samples for FTIR-ATR experiments, a 10-wt. % solution of the VA/VBu copolymer in 1-butanol was cast onto

Table 2. Molecular Weights, Boiling Temperatures, Densities, and Lennard-Jones Diameters for Penetrants

Penetrant	MW (g/mol)	T_b (°C)	ρ (g/cm^3)	σ (Å)
MEK	72.11	80	0.805	4.750*
CH_2Cl_2	84.93	40	1.316	4.759**

*Brokaw (1969).
**Braune and Linke (1930).

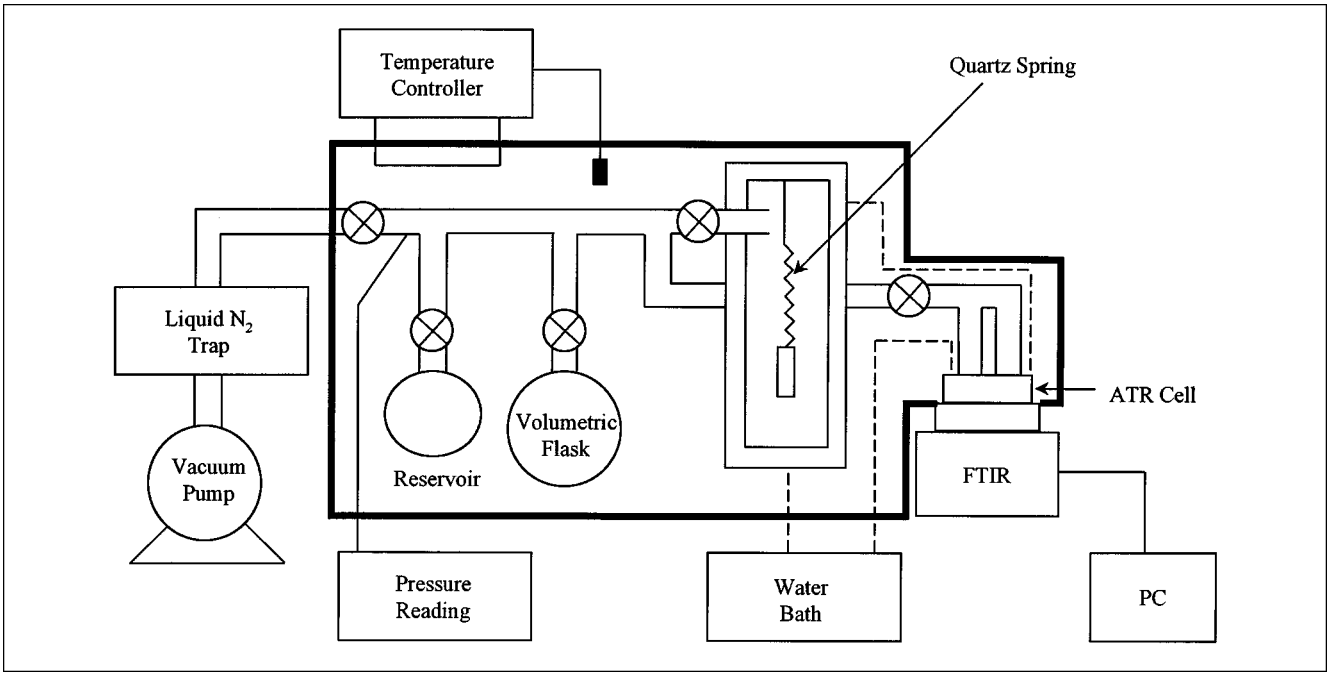

Figure 4. Combined gravimetric sorption and FTIR-ATR apparatus.

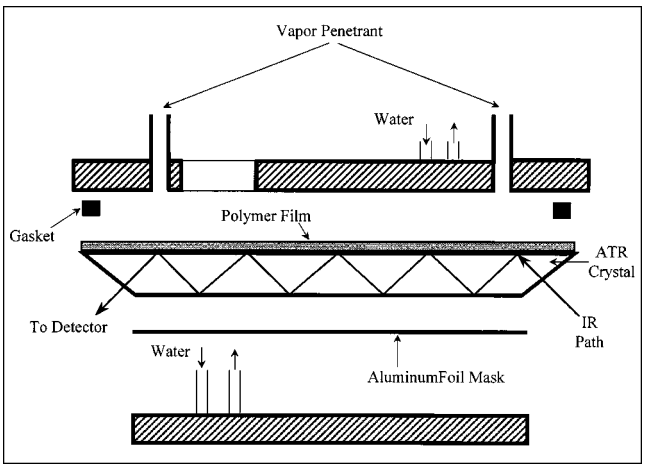

Figure 5. ATR cell.

a level ATR crystal. The polymer film samples were dried for 48 h in a fume hood and then placed in a vacuum oven for 48 h at 125°C to remove residue solvent. The thickness (L) of the samples prepared for spectroscopic experiments was measured using a micrometer and was in the range of 30 to 80 μm (± 2.5 μm).

Diffusion experiments

Figure 4 shows the apparatus used to conduct FTIR-ATR and gravimetric experiments. The penetrant vapor pressure (activity) was controlled by the heating element inside the insulated chamber. Only low vapor activities of penetrant, 0.1 to 0.3, were examined in this study. A temperature-controlled water bath regulated the experimental temperature by circulating water through the glass jacket around the quartz spring and through the ATR cell. All experiments were conducted at 80 ± 0.1°C, which was above the glass transition temperatures of both polymers investigated (see Table 1).

Infrared spectra for the diffusion experiments were obtained with a Mattson Research Series 1 FTIR spectrometer with a horizontal ATR cell (Figure 5) purchased from Graseby Specac, Inc. The ATR crystal (Graseby Specac, Inc.) used in this study was a zinc selenide trapezoid ($70 \times 10 \times 6$ mm), with entry and exit beveled faces at a 45° angle of incidence for the IR beam and a refractive index of 2.4. The sampling parameters for the FTIR-ATR experiments are provided in Table 3. Gravimetric sorption experiments were conducted to determine the equilibrium weight fraction of penetrant coinciding with each FTIR-ATR experiment. For gravimetric experiments, the polymer film was prepared in an aluminum mold and hung directly on the quartz spring. The weight gain of the polymer sample was determined from the spring extension using a cathetometer. Further details about the experimental apparatus and procedures are described elsewhere (Hong et al., 1997).

Results and Discussion

Several infrared spectra, representing the C=O absorbance for MEK in the 11-wt. % VA copolymer during a diffusion experiment at an activity of 0.286, are shown in Figure 6. The breadth of the MEK carbonyl peak in this figure was more than twice that observed in a previous study of MEK diffusion in polyisobutylene (Hong et al., 1997), suggesting hydrogen bonding between the C=O in MEK and the OH in the VA/VBu copolymer. To quantify the hydrogen-bound and free carbonyl absorbances of MEK, the spectra were fit using two Lorentzian contours (Elabd and Barbari, 2000), as shown in Figure 7 for the spectrum at equilibrium. The carbonyl peaks at 1711 cm^{-1} and 1722 cm^{-1} represent the hydrogen-bound and free carbonyl groups, respectively. The location of the free carbonyl stretching band at 1722 cm^{-1} is consistent with an earlier study (Hong et al., 1997), in which the location of the carbonyl stretch for MEK in polyisobutylene was at 1722 cm^{-1}.

The spectra were deconvoluted at each time point during a diffusion experiment using a peak fitting algorithm in the software, Advanced FIRST (Mattson Instruments, Inc.), to determine the integrated absorbances (Elabd et al., 2001). In Figure 8, the relationship between the integrated absorbances for both species, hydrogen-bound and free MEK, is shown for the same diffusion experiment at an activity of 0.286. The linear relationship verifies the local equilibrium assumption, and KC_B^o (see Eq. 22) can be determined from a linear regression of the data. The values of KC_B^o, determined from the diffusion experiments at all activities in this study, were 1.00 ± 0.08 and 1.56 ± 0.19 for the 11- and 19-wt. % VA copolymers, respectively. Figure 9 shows the integrated ab-

Table 3. Sampling Parameters Used in FTIR-ATR Experiments

Parameter	Value
Resolution	4 cm^{-1}
Starting wave number	600 cm^{-1}
Ending wave number	4000 cm^{-1}
Sample scans	32
Signal gain	1
Forward-scan velocity	0.6 cm/s
Reverse-scan velocity	1.3 cm/s
Sampling time	46 s

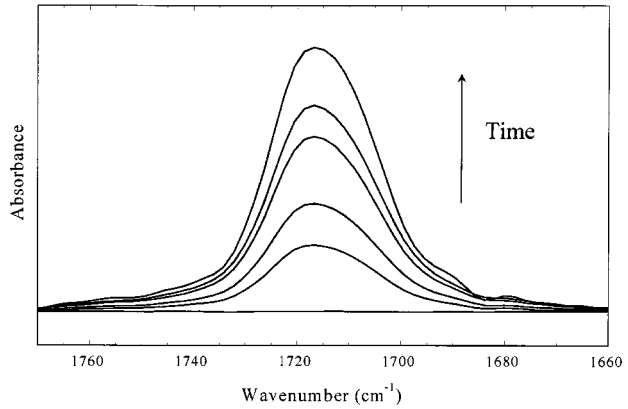

Figure 6. Time-evolved carbonyl absorbance spectra of MEK in 11 wt. % VA/VBu at 80°C and an activity of 0.286.

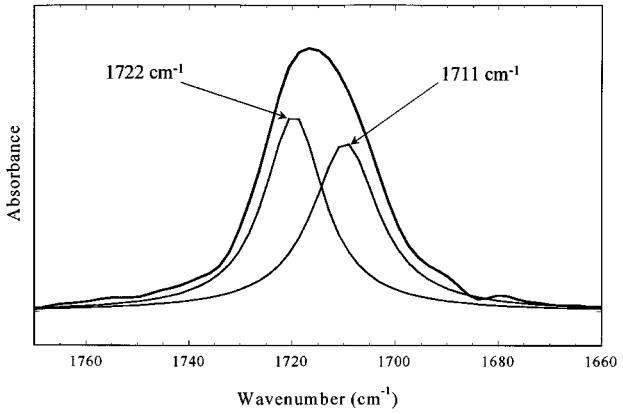

Figure 7. Example of deconvolution of carbonyl absorbance spectrum using Lorentzian contours.

Hydrogen-bound and free carbonyl groups are represented at 1,711 cm^{-1} and 1,722 cm^{-1}, respectively.

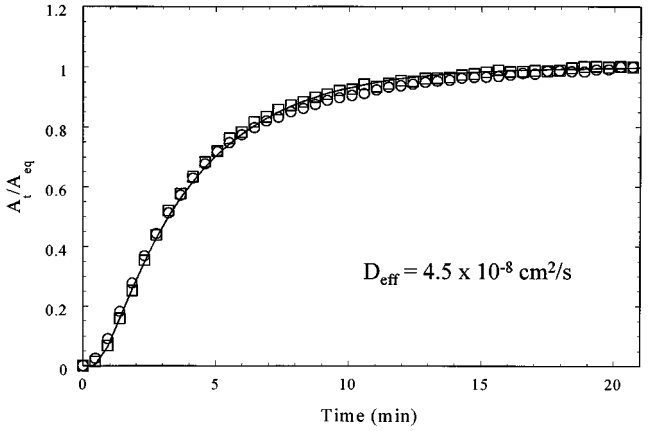

Figure 9. FTIR-ATR data for diffusion of hydrogen-bound (circles) and free MEK (squares) at 80°C and an activity of 0.286 in 11 wt. VA/VBu.

The data were regressed to a Fickian model represented by the solid line.

sorbances for each species plotted as a function of time for the experiment at an activity of 0.286. The transport behavior was Fickian at this activity and at all vapor activities studied for both polymers. Figure 9 also shows the regressed fit of the data using Eq. 20, indicated by the solid line, from which the effective diffusion coefficient was determined. Whether the free or hydrogen-bound MEK is monitored, the data confirm that either Eq. 9 or Eq. 10 can be used to obtain D_{eff}.

The true diffusion coefficient, D_A, can be determined from the equilibrium constant (KC_B^o) and the effective diffusion coefficient (D_{eff}) using Eq. 11. Figure 10 shows the effective and true diffusion coefficients of MEK in the 11- and 19-wt. % VA copolymers, over all the vapor activities studied, plotted here in terms of MEK volume fraction at equilibrium. The diffusion coefficients increase with increasing volume fraction of MEK in the copolymer. The volume fractions were calculated from the weight fractions that were measured gravimetrically, assuming no volume change of mixing for polymers above the glass transition. The results in Figure 10 agree with simple free volume theory (Cohen and Turnbull, 1959; Macedo and Litovitz, 1965; Chung, 1966). Solvation hinders the diffusion of MEK in the VA/VBu copolymers by

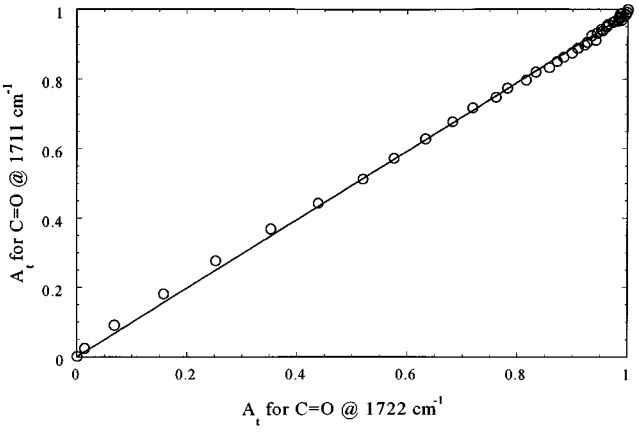

Figure 8. Integrated absorbances of hydrogen-bound and free carbonyl groups at 80°C and an activity of 0.286 in 11 wt. % VA/VBu.

Solid line represents fit, assuming local equilibrium (Eq. 8).

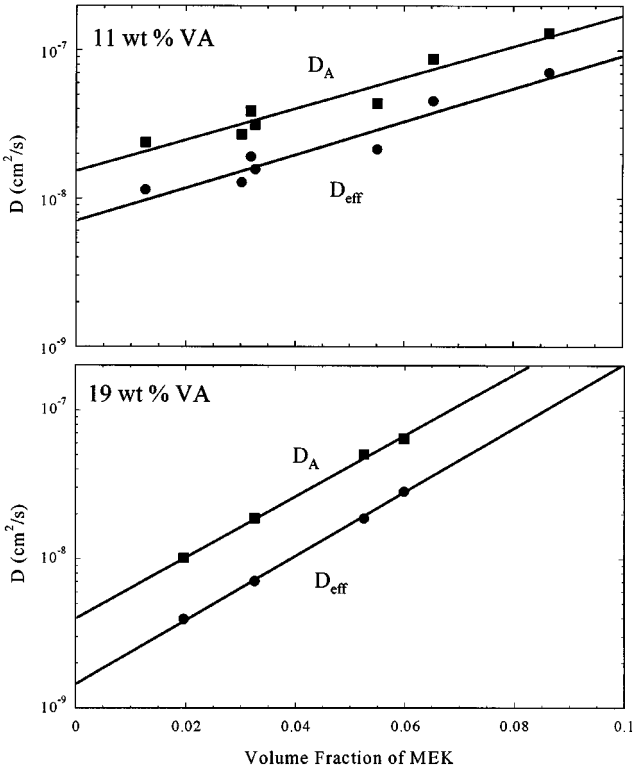

Figure 10. Effective (circles) and true (squares) diffusion coefficients for MEK in the VA/VBu copolymers.

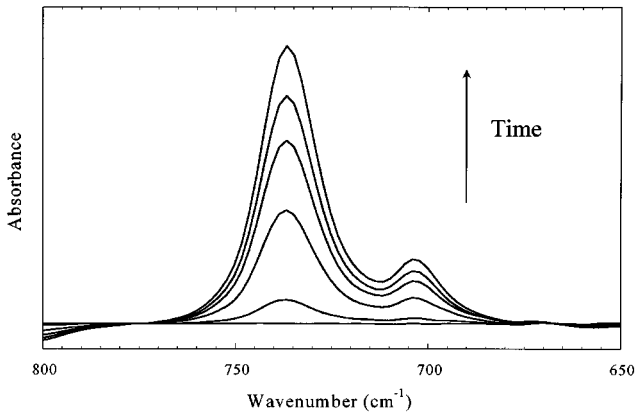

Figure 11. Time-evolved C-Cl spectra for CH_2Cl_2 in 11 wt. % VA/VBu at 80°C and an activity of 0.215.

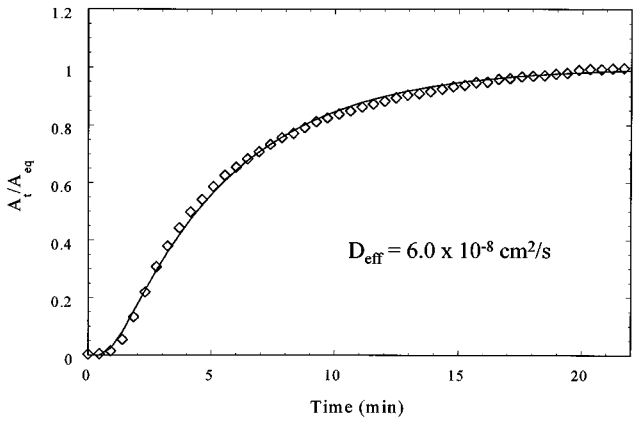

Figure 12. FTIR-ATR data for diffusion of CH_2Cl_2 in 11 wt. % VA/VBu at 80°C and an activity of 0.215.

The data were regressed to a Fickian model represented by the solid line.

factors of 2.0 (11-wt. % VA) and 2.6 (19-wt. % VA). The hindrance effect increases with increasing VA content in the polymer because the equilibrium between free and hydrogen-bound states shifts to favor more hydrogen bonding (higher C_B^o). If C_B^o is separated from KC_B^o in the two copolymers, then K should be constant and independent of VA content. The values of C_B^o for the 11- and 19-wt. % VA copolymers are 2.71 M and 4.83 M, respectively. The resulting values of K are 0.37 ± 0.03 M^{-1} and 0.32 ± 0.04 M^{-1} for 11- and 19-wt. % VA, respectively.

To test the hypothesis that the diffusion coefficients of solvating and nonsolvating penetrants of equal size are the same after accounting for solvation, diffusion coefficents were measured for methylene chloride and compared with the true values for MEK. Methylene chloride (CH_2Cl_2) was chosen because it has considerably weaker interactions with the VA/VBu copolymers than does MEK and has a similar Lennard-Jones diameter (see Table 2). Figure 11 shows time-evolved spectra of the C-Cl stretch of CH_2Cl_2 in the 11-wt. % VA copolymer during a diffusion experiment at an activity of 0.215. Two peaks are evident at 737 cm^{-1} and 704 cm^{-1}, both of which represent the C−Cl bond and appear in the spectrum of pure CH_2Cl_2 at the same locations. The integrated absorbance at each time point, the total area under both peaks, is plotted in Figure 12 for the same experiment, and the diffusion coefficient was determined with the method described earlier. Figure 13 compares the diffusion coefficients of CH_2Cl_2 with the true diffusion coefficients of MEK from Figure 10 at all of the volume fractions studied. In both polymers, there is excellent agreement between the CH_2Cl_2 diffusion coefficients and the true diffusion coefficients of MEK determined from the solvation model in this study, validating the stated hypothesis.

Conclusion

FTIR-ATR spectroscopy is a powerful tool for the measurement of both equilibrium constants and diffusion coefficients in polymers because of its ability to examine strong interactions between a penetrant and the polymer through shifts in the infrared spectrum. Although the equilibrium constants measured here could have been obtained from equilibrium sorption experiments using infrared spectroscopy, their determination from time-evolved spectra during the diffusion process allows the validity of the local equilibrium assumption to be tested. Its validity was demonstrated here by the reproducible value of the equilibrium constant, K, measured at all concentrations, at all times, and for both copolymers. Rather than using total mass to determine the effective diffusion coefficient for a solvating pene-

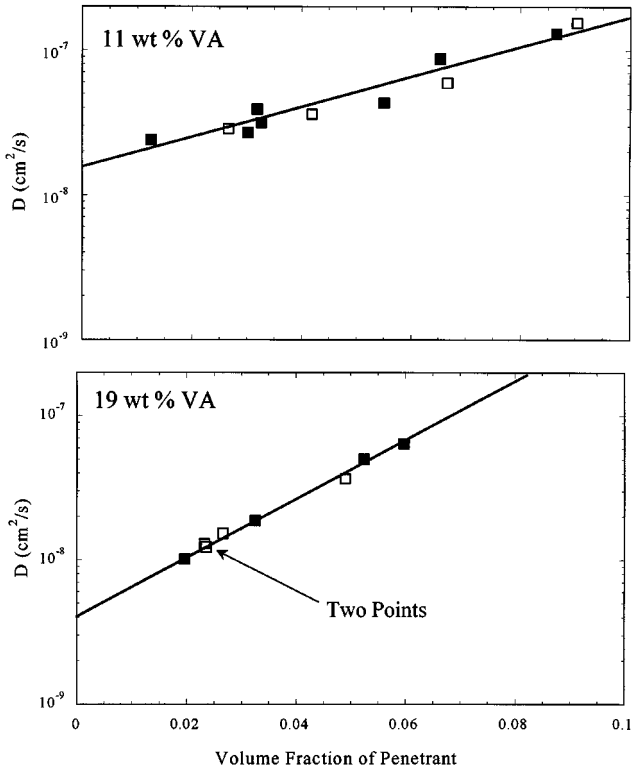

Figure 13. True diffusion coefficients: MEK (solid squares) vs. CH_2Cl_2 (open squares).

trant, as in gravimetric techniques, FTIR-ATR spectroscopy can monitor the individual species present. This ability is invaluable for systems in which local equilibrium may no longer be valid, such as glassy polymers.

Separating the effect of hydrogen bonding from the effective diffusion coefficient of MEK in the VA/VBu copolymers gives a true diffusion coefficient for the penetrant. The diffusion-solvation model developed here was verified by the finding that the true diffusion coefficients for MEK were the same as those for methylene chloride, a penetrant of similar size.

Acknowledgment

The authors acknowledge the financial support of the U.S. Army Research Office through Grant DAAD19-00-1-0009 at the University of Maryland, and the Army Research Laboratory Materials Center of Excellence at Johns Hopkins University through Grant DAAL01-96-2-0047.

Literature Cited

Barbari, T. A., S. S. Kasargod, and G. T. Fieldson, ''Effect of Unequal Transport Rates and Intersolute Solvation on the Selective Batch Extraction of a Dilute Mixture with a Dense Polymeric Sorbent,'' *Ind. Eng. Chem. Res.*, **35**, 1188 (1996).

Bartlett, P. N., and J. W. Gardner, ''Diffusion and Binding of Molecules to Sites Within Homogeneous Thin Films,'' *Philos. Trans. R. Soc. London A.*, **354**, 35 (1996).

Braune, H., and R. Linke, ''The Viscosity of Gases and Vapors: III. Influence of the Dipole Moment on the Magnitude of the Sutherland Constant,'' *Z. Phys. Chem.*, **A148**, 195 (1930).

Brokaw, R. S., ''Predicting Transport Properties of Dilute Gases,'' *Ind. Eng. Chem. Process Des. Dev.*, **8**, 240 (1969).

Chung, H. S., ''The Macedo-Litovitz Hybrid Equation for Liquid Viscosity,'' *J. Chem. Phys.*, **44**, 1362 (1966).

Cohen, M. H., and D. J. Turnbull, ''Molecular Transport in Liquids and Glasses,'' *J. Chem. Phys.*, **31**, 1164 (1959).

Elabd, Y. A., J. M. Sloan, and T. A. Barbari, ''Diffusion of Acetonitrile in Conformational Isomers of an H_{12} MDI Polyurethane,'' *Polymer*, **41**, 2203 (200).

Elabd, Y. A., and T. A. Barbari, ''Diffusion of Acetic Acid in Polyisobutylene: Probing Small Molecule Structures,'' *Ind. Eng. Chem. Res.*, in press (2001).

Fieldson, G. T., and T. A. Barbari, ''Analysis of Diffusion in Polymers Using Evanescent Field Spectroscopy,'' *AIChE J.*, **41**, 795 (1995).

Harrick, N. J., ''Electric Field Strengths at Totally Reflecting Interfaces,'' *J. Opt. Soc. Amer.*, **55**, 851 (1965).

Harrison, M., and B. P. Hills, ''Mathematical Model of Flavor Release from Liquids Containing Aroma-Binding Macromolecules,'' *J. Agric. Food Chem.*, **45**, 1883 (1997).

Hermans, J. J., ''Diffusion with Discontinuous Boundary,'' *J. Colloid Sci.*, **2**, 387 (1947).

Hong, S. U., T. A. Barbari, and J. M. Sloan, ''Diffusion of Methyl Ethyl Ketone in Polyisobutylene: Comparison of Spectroscopic and Gravimetric Techniques,'' *J. Poly. Sci.: Poly. Phys. Ed.*, **35**, 1261 (1997).

Hong, S. U., T. A. Barbari, and J. M. Sloan, ''Multicomponent Diffusion of Methyl Ethyl Ketone and Toluene in Polyisobutylene from Vapor Sorption FTIR-ATR Spectroscopy,'' *J. Poly. Sci.: Poly. Phys. Ed.*, **36**, 337 (1998).

Kim, D., H. Reiss, and H. M. Rabeony, ''Thermodynamically Reversible Uptake of Electrically Active Dopants in Conducting Polymers: Iodine in Polythiophene,'' *J. Phys. Chem.*, **92**, 2673 (1988).

Macedo, P. B., and T. A. Litovitz, ''The Relative Roles of Free Volume and Activation Energy in the Viscosity of Liquids,'' *J. Chem. Phys.*, **42**, 245 (1965).

MacKnight, W. J., and M. Yang, ''Property-Structure Relationships in Polyurethanes: Infrared Studies,'' *J. Poly. Sci. Symp.*, **42**, 817 (1973).

Murphy, W. D., H. M. Rabeony, and H. Reiss, ''Numerical Analysis of Diffusion in the Presence of Nonlinear Reversible Trapping,'' *J. Phys. Chem.*, **92**, 7007 (1988).

Peppas, N. A., and S. L. Wright, ''Drug Diffusion and Binding in Ionizable Interpenetrating Networks from Poly(vinyl alcohol) and Poly(acrylic acid),'' *Eur. J. Pharm. Biopharm.*, **46**, 15 (1998).

Reimers, M. J., M. J. Cibulsky, and T. A. Barbari, ''Gas Sorption and Diffusion in Hydrogen-Bonded Polymers. I. Vinyl Alcohol/Vinyl Butryal Copolymers,'' *J. Poly. Sci.: Poly. Phys. Ed.*, **31**, 537 (1993).

Senich, G. A., and W. J. Macknight, ''Fourier Transform Infrared Thermal Analysis of a Segmented Polyurethane,'' *Macromolecules*, **13**, 106 (1980).

Sjöberg, H., S. Persson, and N. Caram-Lelham, ''How Interactions Between Drugs and Agarose-Carrageenan Hydrogels Influence the Simultaneous Transport of Drugs,'' *J. Control. Relat.*, **59**, 391 (1999).

Sung, C. S. P., and N. S. Schneider, ''Structure-Property Relationships of Polyurethanes Based on Toluene Diisocyanate,'' *J. Mater. Sci.*, **13**, 1689 (1978).

Teo, L. S., C. Y. Chen, and J. F. Kuo, ''Fourier Transform Infrared Spectroscopy Study on Effects of Temperature on Hydrogen Bonding in Amine-Containing Polyurethanes and Poly(urethane-urea)s,'' *Macromolecules*, **30**, 1793 (1997).

Wang, C. B., and S. L. Cooper, ''Morphology and Properties of Segmented Polyether Polyurethaneureas,'' *Macromolecules*, **16**, 775 (1983).

Manuscript received Feb. 28, 2000.